# CHARACTERIZATION OF SUB-MICROMETER FEATURES WITH THE FE-EPMA

Peter McSwiggen

McSwiggen & Associates, 2855 Anthony Lane South, Suite B1
St. Anthony, Minnesota, U.S.A. 55418-2883 PMcS@McSwiggen.com

McSwiggen received his first degree in Geology from the University of Minnesota (Bachelor of Science), followed by a M.S. from the University of Maine, and a Ph.D. from University of Minnesota. He went to work for the Minnesota Geological Survey for ten years before taking over the management of the electron microprobe lab in the Department of Geology at the University of Minnesota. In 1997, he started to consult for JEOL USA providing electron microprobe training for their new customers. In 2003 he started his own electron microprobe service company. To date, he has published 25 scientific articles, maps and reports of investigations, and an additional 24 abstracts.

## 1. ABSTRACT

The goal of this work is to compare two strategies for doing sub-micron analyses using the Fe-Ni binary system, as an example. The first approach involves reducing the overvoltage to the minimum required to preform the analysis, while still using the K-lines. Using an accelerating voltage, just slightly higher than the critical ionization energy for the K-lines, restricts the size of the analytical volume. The beam electrons will quickly lose their small overvoltage energy, making it possible to produce the K X-ray lines only a very short distance from the surface. The second strategy is to use the L-lines for Fe and Ni, and drop the accelerating voltage to a level that will produce the smallest overall interaction volume of the beam electrons. Each strategy has its advantages and disadvantages that depend on the ultimate goal of the analysis and the elements involved in the analysis.

## 2. INTRODUCTION

The field emission electron column has dramatically changed electron imaging. The higher electron density and smaller electron energy spread allows for an electron beam spot size that is an order of magnitude smaller than that produced by the traditional thermionic tungsten filament. This smaller spot size results in images that have far improved spatial resolution, particularly at high beam currents (Fig. 1). Earlier cold field emission electron guns were not suitable for the electron microprobe because of their poor beam stability

(~10%/hour) and their low beam currents (~ $1x10^{-9}$ amp). With the thermal, field emission electron guns (TFE), both beam stability (< 0.1%/hour) and high beam currents (~ $1x10^{-6}$ amp) can be achieved. This now makes the field emission gun ideal for the electron microprobe.

Some have previously argued that the field emission gun does not add to the analytical range of the electron microprobe because the electron spread within the sample controls the analytical area, not the beam diameter. The electron spread is controlled by the energy of the electron beam and the density/atomic number of the sample being analyzed. However, with the thermal, field emission (TFE) electron gun, it is possible to work at much lower accelerating voltages and still maintain a very small spot size. This greatly reduces the analytical area.

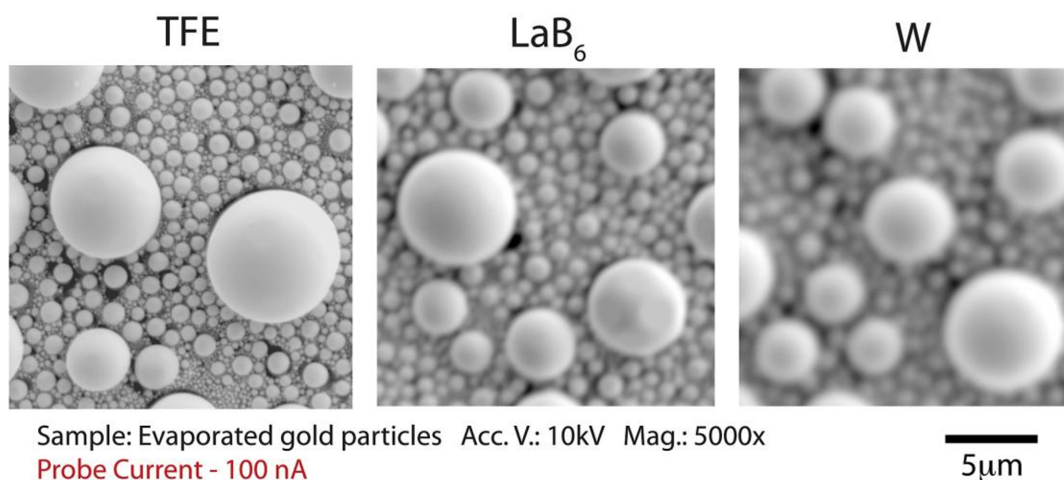


Figure 1. Differences in imaging between a thermionic W filament gun (W), a $LaB_6$ gun, and a thermal field emission gun (TFE). Sample is evaporated gold particles on carbon. (Imaging by JEOL, Ltd.)

It should be pointed out that high-resolution imaging can also greatly improve the quality of microanalyses, even if one is not working at low-accelerating voltages. High spatial resolution imaging not only assists in determining what to analyze, but helps identify where not to analyze. Figure 2 is an example. Shown are small crystallites in a volcanic glass. If the objective is to analyze the glass, it is critical to be able to identify areas where the crystallites exist in order to avoid them. Therefore, even if the analytical volume is much larger than the size of the crystallites, finding larger areas clear of them becomes paramount.

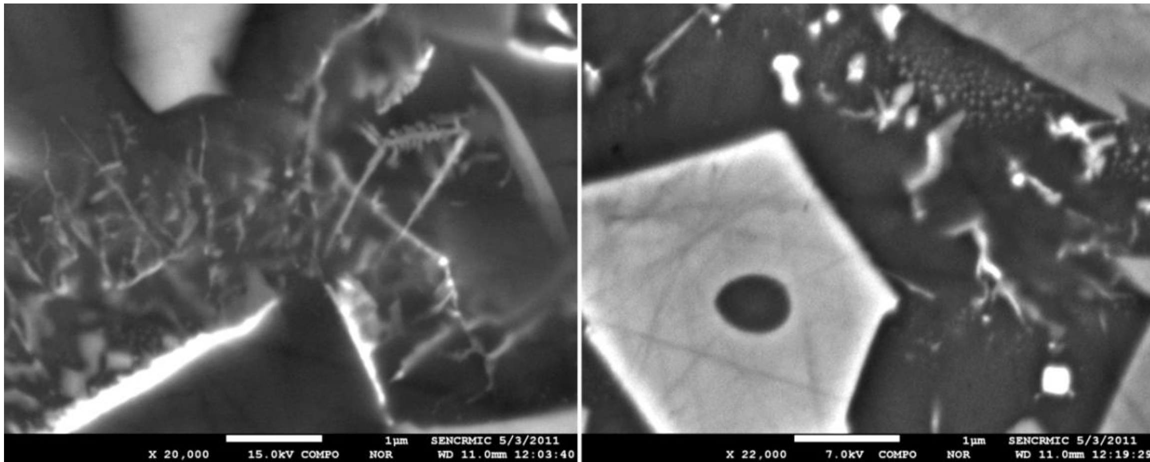


Figure 2. Backscattered electron images of sub-micron dendritic crystallites in a volcanic glass collected on a JEOL 8530F field emission electron microprobe. The crystallites are too small to analyze, but high-resolution imaging means that they can be avoided when preforming analyses of the glass.

Two general strategies have been suggested for analyzing very small volumes (Armstrong, 2011) (1) low voltage analyses, and (2) low overvoltage analyses. Both have advantages and disadvantages. This work will attempt to summarize the many issues that should be considered when attempting to decide which approach is best for a given analytical situation. These include: (1) the size of the analytical volumes, (2) minimum detection limits, (3) quality of the matrix corrections, (4) secondary fluorescence, (5) effects of surface contamination, oxide layers, and carbon coatings.

## 3. LOW VOLTAGE ANALYSES (low kV)

As one decreases the accelerating voltage, and therefore the energy of the beam electrons, the spread of the electron within the sample is also reduced. The electrons have less energy and therefore can travel only a short distance before they have lost all of their energy. Therefore, one can greatly reduce the size of the area being analyzed by dropping the accelerating voltage (Fig. 3) from the typical microprobe analytical range of 15-25 kV to a low voltage range of 5-10 kV. Often, this will also mean switching to a lower energy X-ray line. However, there is a limit as to how low the accelerating voltage can be decreased and still improve the spatial resolution of the analyses. As the accelerating voltage is decreased, the interaction volume decreases, but the diameter of the electron beam increases (Fig. 4). Therefore, there is an optimum accelerating voltage for each material, where the size of the area of electron scattering within the sample is equal to the diameter of the beam. A lower

accelerating voltage will increase the analytical area because the beam diameter is bigger, and a higher accelerating voltage will increase the analytical areas because of a larger scatter volume. The optimum accelerating voltage depends on the material, but typically falls in the 5 to 8 kV range.

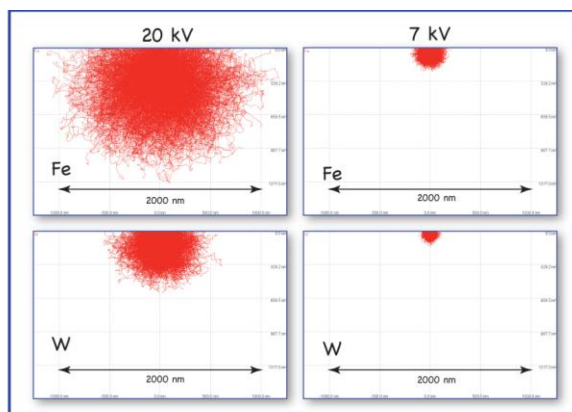


Figure 3. Monte Carlo modeling shows the improved spatial resolution with both increased atomic number and a decrease in the accelerating voltage. The diameter of the interaction volume for Fe drops from 2000 nm at 20 kV to about 300 nm at 7 kV. For W, the diameter drops from about 1000 nm at 20 kV to about 160 nm at 7 kV. (Models generated by CASINO).

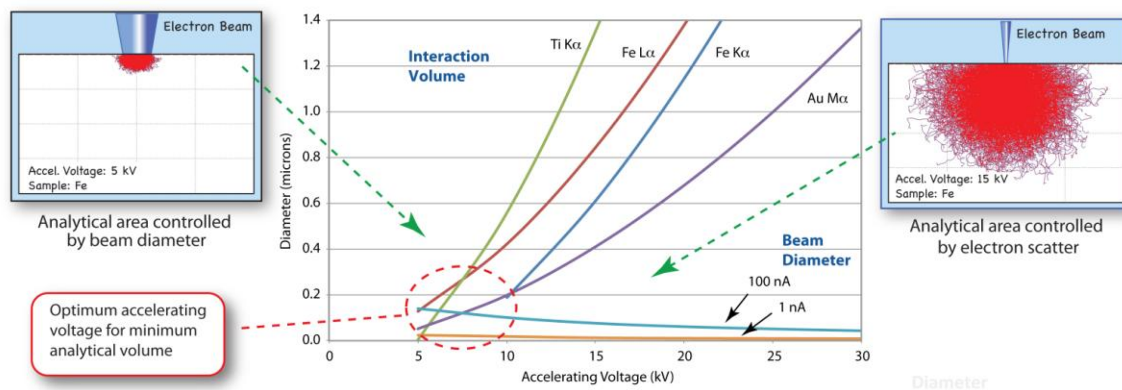


Figure 4. The analytical area is controlled by both the beam diameter and the scatter within the sample. For every material there is an optimum accelerating voltage that will produce the minimum analytical area. Commonly, this is in the 5 to 8 kV range. At a higher accelerating voltage, scattering within the sample generates a larger analytical area; at a lower accelerating voltage the expanding beam diameter makes for a larger analytical area. The beam diameter was measured on JEOL JXA-8530F field emission electron microprobe.

## 4. LOW OVERVOLTAGE ANALYSES (low-U)

A second method that can be used to generate a small analytical volume is to minimize the overvoltage (U) (U = accelerating voltage / critical ionization energy of X-ray) (Armstrong, 2011). Typically an overvoltage of around 2 is recommended for routine analyses. This gives each beam electron enough energy to generate at least one characteristic X-ray, even if it has lost considerable energy due to other types of inelastic interactions within the sample. However, this high overvoltage results in considerable scattering of the beam electrons within the sample, making a large volume from which the X-rays will be generated.

A low overvoltage analysis reduces the accelerating voltage to the minimum required to produce the characteristic X-ray of interest. An accelerating voltage of just 1-3 kV over the critical ionization energy is used. This dramatically reduces the number of X-rays generated, but also greatly reduces the volume from which the X-rays will be produced. The total electron interaction volume can still be very large, but the beam electrons quickly lose the required energy to create the characteristic X-rays of interest. As a result, all of the X-rays of interest are generated from a small volume near the surface (Fig. 5).

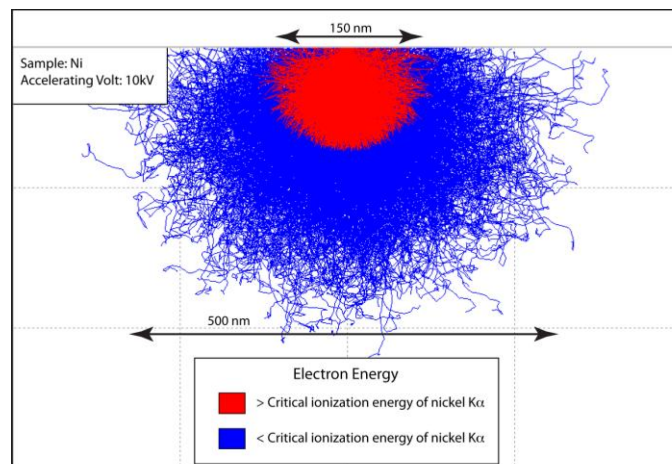


Figure 5. Shown are Monte Carlo simulations of the size of the total electron interaction volume within Ni metal (blue) for a 10 kV accelerating voltage. Compared to that is the volume in which the electrons have enough energy (8.332 keV) to produce Ni Kα X-rays (analytical volume in red). As the 10 keV electrons scatter within the sample, they quickly lose sufficient energy to produce the Ni Ka X-rays, resulting in a small analytical volume.

Both the low voltage method and the low overvoltage method for analyzing sub-micron areas have advantages and disadvantages. The remainder of the paper will evaluate one binary system (Fe-Ni) in order to compare the differences between the two approaches. The purpose is not to determine which method is better overall. That will depend on the material being analyzed and the objective of the analyses. For a given material, one method might work better for map analysis, while the other for quantitative analysis. One method might be better for the detection limits in trace element analyses, the other for accuracy in major element analyses. The objective is to highlight some of the issues that should be considered when attempting to achieve the smallest analytical volumes.

For the low U analysis, 10 kV was selected for the accelerating voltage. This is only 1.7 kV higher than the critical ionization energy required to produce the Ni Kα X-ray line (Table 1). A lower accelerating voltage would reduce the number of Ni Kα X-rays generated to a level less than acceptable. The alternative is to use the L-lines for Ni and Fe. The critical ionization energy for these X-ray lines would, in theory, allow for an accelerating voltage as low as 1 kV to be used. However, considering the issues discussed in Figure 4, and others to be discussed later, the low kV analyses for this work will be limited to 7 kV.

Table 1. Critical ionization energy of Fe and Ni X-ray lines (Goldstein, et al. 1992).

| | K□(□□□) | L□(□□□) |
|---|---|---|
| Fe | 7.111 | 0.707 |
| Ni | 8.332 | 0.854 |

5. ANALYTICAL VOLUMES

Monte Carlo modeling can be used to determine the size of the volume in which X-rays are generated by simply putting a threshold on the electrons, truncating the path once they have dropped below the critical ionization energy of the X-ray in question. A comparison of the X-ray generation volumes for the low U analysis method (using Fe Kα, Ni Kα and 10 kV) and the low kV analysis method (Fe Lα, Ni Lα, and 7 kV) is shown in Figure 6.

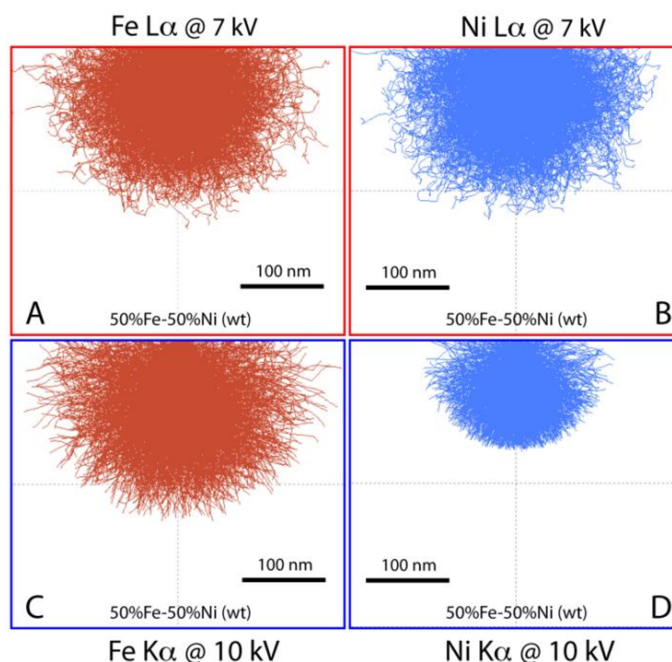


Figure 6. Monte Carlo modeling of the analytical volume for Fe Lα and Ni Lα X-ray lines at 7 kV, and Fe Kα and Ni Kα X-ray lines at 10 kV for a metal containing 50 wt.% Fe and 50 wt.% Ni. These volumes were determined from the electron interaction volumes truncated at the critical ionization energy for the X-ray line in question. (Models generated using CASINO)

For both Fe and Ni, the volume in which the L-lines can be generated at 7 kV in a metal containing 50 wt.% Fe and 50 wt.% Ni (Fig. 6A-B), is about 200 nm in diameter. For the K-lines at 10 kV, the Fe volume is also about 200 nm in diameter (Fig. 6C), whereas the Ni volume is closer to about 150 nm (Fig. 6D). The depths from which the X-rays can escape are generally smaller than the diameter of the X-ray generation volume. The phi-rho-Z plots in Figure 7 show the depths at which the various X-rays are generated, and from which the X-rays can escape. For the K-lines, these two profiles are nearly identical. For the L-lines, there is a significant difference.

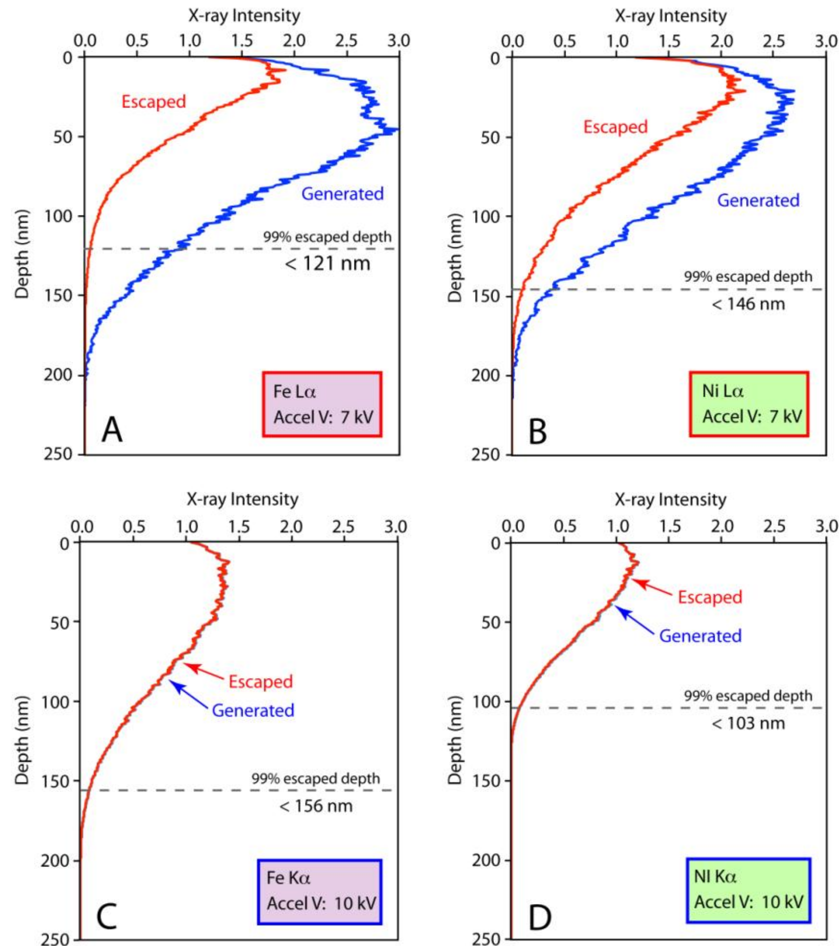


Figure 7. Phi-rho-Z plots for Fe Lα, Ni Lα, Fe Kα and Ni Kα in a material consisting of 50 wt.% Fe and 50 wt.% Ni. The dashed lines on each plot show the depth above which 99% of the escaped X-rays will come.

Due to the low energy of the L-lines, there is a large discrepancy between the number of X-rays generated in the sample and the number that ultimately escape from the surface (Fig. 7A-B). The sample absorbs many of the generated X-rays before they reach the surface. This discrepancy must be corrected for by the matrix correction routines. These large corrections are one of the reasons for the errors when using the lower energy L-lines in quantitative analyses. Because of the higher energy of the K-lines, most of the generated Kα X-rays for Fe and Ni will escape; therefore, the matrix corrections are much smaller.

The analytical depth for these X-ray lines in a metal that is 50:50 Fe:Ni can be defined using the 99% escaped depths show in Figure 7. This is the depth above which 99% of the escaped X-rays came. For Fe Lα and Ni Lα this is between about 120 to 150 nm. For Fe

Kα this depth is about 156 nm, and for Ni Kα it is about 100 nm. Therefore there is not a huge difference in the analytical area between the low kV and the low U analytical method for the Fe-Ni binary. Both should allow for analyses of volumes that are in the range of about 200 nm in diameter, and about 150 nm in depth. This is similar to the empirical observations of McSwiggen, et al. (2011), where they report consistent quantitative analyses of $Ag_3Sn_1$ grains down to about 250 nm.

## 6. SECONDARY FLUORESCENCE

X-rays can be generated in a sample from more than just the beam electrons. In many samples, secondary fluorescence can also generate characteristic X-rays. X-rays produced by the primary electrons can fluoresce X-rays in another phase some distance from the primary electron interaction volume. These secondary X-rays are then mistakenly assumed to be coming from the phase being analyzed (Fournelle, 2007; Fournelle, et al., 2005). Whether a secondary X-ray is fluoresced depends mostly on the energy of the primary X-ray relative to the critical ionization energy of the secondary X-ray. The probability of fluorescence is at its greatest when the energies are the same. As the difference between the two energies increases, the probability of fluorescence decreases. If the primary X-ray has an energy greater than the critical ionization energy of the secondary X-ray of more than about 3 keV, then there will be no significant fluorescence (Goldstein, et al., 1992, p. 141). If the primary X-ray has less energy than the critical ionization energy of the secondary X-ray, then it is not possible to create the secondary fluorescence.

To determine the degree to which secondary fluorescence may be a problem in the Fe-Ni system, the NIST program DTSA II was used to model the effect. It was assumed that an area of pure nickel was in contact with a pure iron metal phase. Spectra were generated for spots within the Ni phase at various distances from the interface with the Fe. The weight percent of Fe was determined using both the Fe Kα line and the Fe Lα line. The results are shown in Figure 8. When the Fe Kα line is used, one can see that the effect of secondary Fe fluorescence is very significant. Even 10 to 20 microns from the interface, about 0.5 wt.% Fe could be measured. This would be a major problem if trying to measure minor or trace concentrations of Fe in a nickel phase that was surrounded by an iron phase. However, Figure 8B shows that if the Fe Lα line is used, no Fe was detected beyond about 0.2 microns from the interface when a 7 kV accelerating voltage was used. Therefore, a sub-micron grain of nickel, surrounded by an iron phase, could still be analyzed for trace amounts of Fe. The reason there is little fluorescence of the Fe Lα line is that the energy of the Fe Kα and Ni Kα lines are too high to fluoresce a Fe Lα line, and the energy of the Ni Lα is too low to allow it to travel very far within the sample.

The Fe-Ni system is particularly sensitive to secondary fluorescence when using the K-lines. Other systems would have to be evaluated individually to determine the importance of this process when analyzing sub-micron grains.

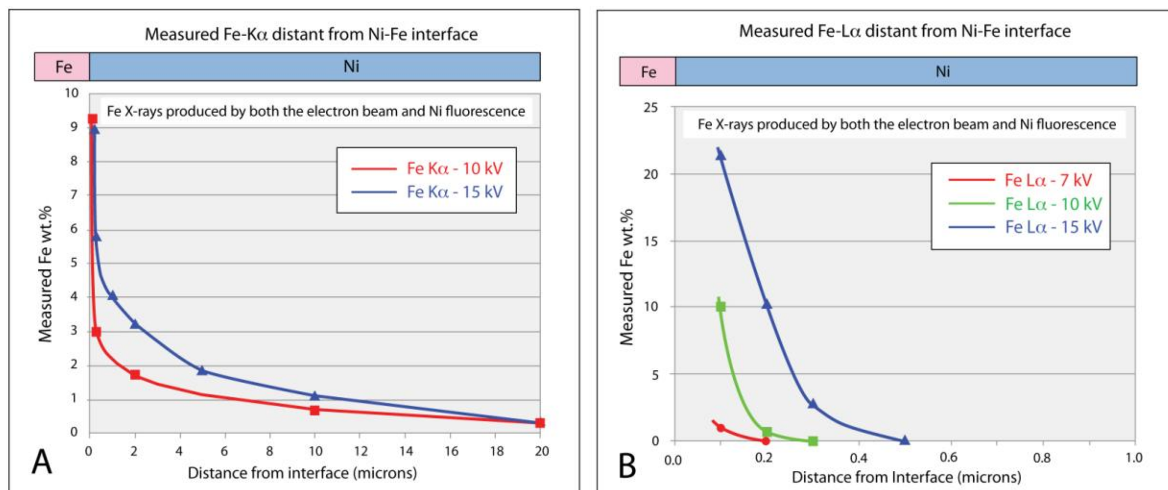


Figure 8. Plots showing the measured Fe resulting from secondary fluorescence when analyzing Ni metal near an interface of Fe, using Fe Kα (A) and Fe Lα (B) X-ray lines. Even 10 to 20 microns from the surface, 0.5 wt.% Fe can be measured if the Fe Kα lines are used and a 10 kV accelerating voltage. If the Fe Lα line is used, no measureable Fe can be detected past 0.2 microns from the interface. Modeling was done using the NIST program DTSA II.

## 7. DETECTION LIMITS

Both methods for analyzing small volumes, whether using a low kV or using a low overvoltage will result in a drop in X-ray counts. As the accelerating voltage is reduced, each beam electron is capable of producing fewer X-rays. This in turn reduces the detection limits for the element in question. Figure 9 shows the calculated detection limits for Ni Kα and Ni Lα in Fe metal as a function of accelerating voltage. These detection limits were calculated using Equation 1, while keeping the counting time and beam current constant at 20 seconds and 100 nA, respectively. The absolute values shown in Figure 9 are not significant. These will vary with the sensitivity of the spectrometer being used, the counting time, and the beam current. However, if one keeps these constant, the detection limit can degrade precipitously as one tries to minimize the analytical area by dropping the accelerating voltage. For the Ni Kα line, the detection limits become asymptotic as the

accelerating voltage approaches the critical ionization energy (8.332 keV) (Fig. 9A). For the Ni Lα line, the best detection limit is achieved at an accelerating voltage of around 10 to 15 kV (Fig. 9B) The detection limit worsens when the accelerating voltage is either increased or decreased. Decreasing the accelerating voltage produces fewer X-rays, while increasing the voltage will produce more X-rays. However, the X-rays are produced deeper in the sample, thereby getting absorbed before they reach the surface. Therefore the maximum measured Ni Lα X-rays occur at the intermediate accelerating voltage.

It is clear that there is a trade-off between trying to obtain the smallest analytical area and the best detection limits. Attempting to minimize the analytical area will result in a worse detection limit. Comparing a 10 kV Ni Kα analysis with a 7 kV Ni Lα analysis shows that the Ni Lα analysis has the better detection limit for a comparable analytical area. However, for Fe the reverse is true. This is due to the low count rate for Fe Lα on the TAP crystal. Again, every situation is different. Spectrometer performances vary, as do intensities from one element to another. Therefore one cannot generalize to other element systems without preforming the measures on the specific electron microprobe that will be used.

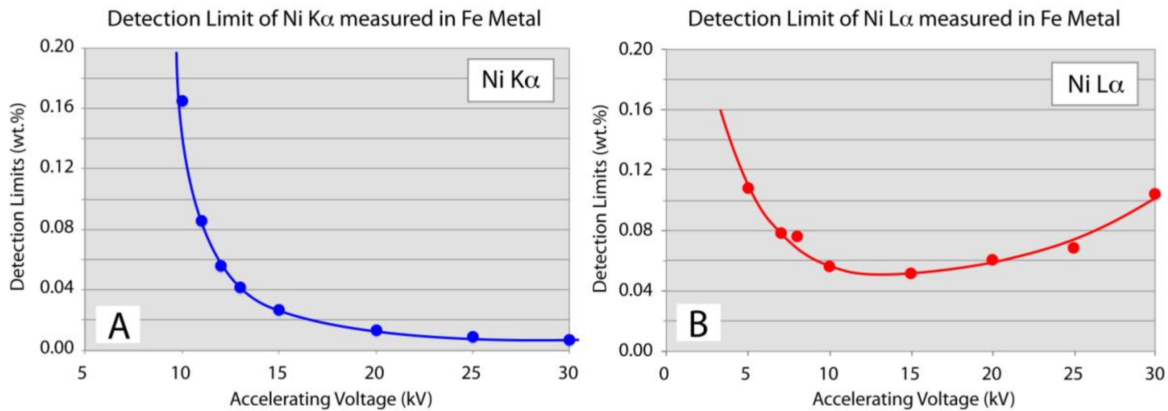


Figure 9. Detection limits for Ni Kα and Ni Lα as a function of accelerating voltage. Values were calculated from measured count rates and Equation 1.

$$MDL = \frac{3\sqrt{I_B}}{I_P} * 100 \qquad (1)$$

where: $I_B$ = intensity of the background in the Ni peak position on Fe metal
$I_P$ = net intensity of the Ni peak on pure Ni

8. QUALITY OF QUANTITATIVE ANALYSES

One problem with low kV analyses is that for many of the transition elements the K X-ray lines can no longer be used, if a 7 kV accelerating voltage is used, and the L lines can be problematic in some cases. For example, Fe has an absorption edge between the Lα and Lβ lines. This absorption edge causes a shift in the combined peak position on a layered synthetic crystal (2d = 6 nm) with changes in Fe abundance. On the TAP crystal, Lα and Lβ peaks are separate, but their mass absorption coefficients are dramatically different and poorly known because of the position of this absorption edge (Armstrong, 2011). For the low energy L lines, this is a particular problem because of the massive absorption that they undergo within the sample. Figure 10 shows a plot of the measured Ni Lα k-ratios at 5 different accelerating voltages for a set of standards along the Fe-Ni binary. At 20 kV, the measured k-ratio for a 50 wt.% Ni standard is about 0.25. About half of the expected X-rays are being absorbed by the sample. At successively lower accelerating voltages, the depth the beam electrons can penetrate diminishes, and therefore, the volume the X-rays are generated in becomes smaller and closer to the surface. Since the path to the surface is shorter, few of the X-rays get absorbed. At a 2 kV accelerating voltage, the Ni Lα k-ratio is equal to the weight ratio of the Ni in the binary sample, and no matrix corrections are required to obtain the correct values. In this case, simply using a sufficiently low accelerating voltage can overcome the uncertainty in the mass absorption coefficient.

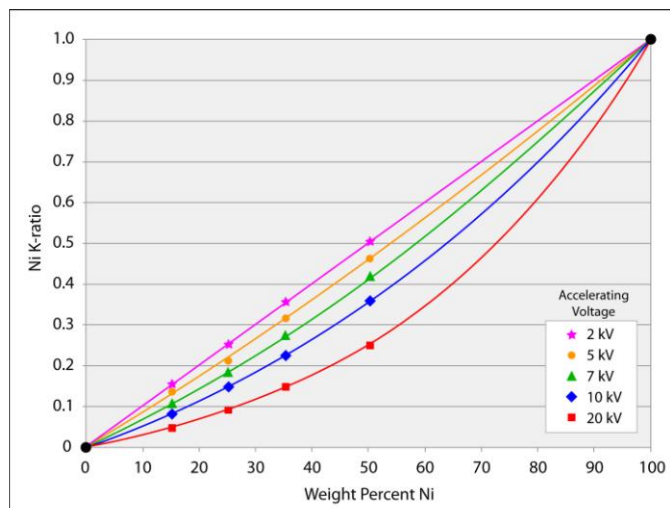


Figure 10. Plot of Ni Lα k-ratios against the Ni wt.% as a function of accelerating voltage for sample along the Fe-Ni binary.

Above a 2 kV accelerating voltage, the matrix corrections perform poorly (Figure 11A) for the L lines. For the Ni Lα line, the matrix correction dramatically over-corrects for the absorption. For the Fe Lα line, the matrix corrections are acceptable between 15 and 25 kV, but they do not properly correct at lower accelerating voltages. The K lines perform much more reliably over the range of accelerating voltages from 10 to 25 kV for both Fe Kα and Ni Kα (Fig. 11B).

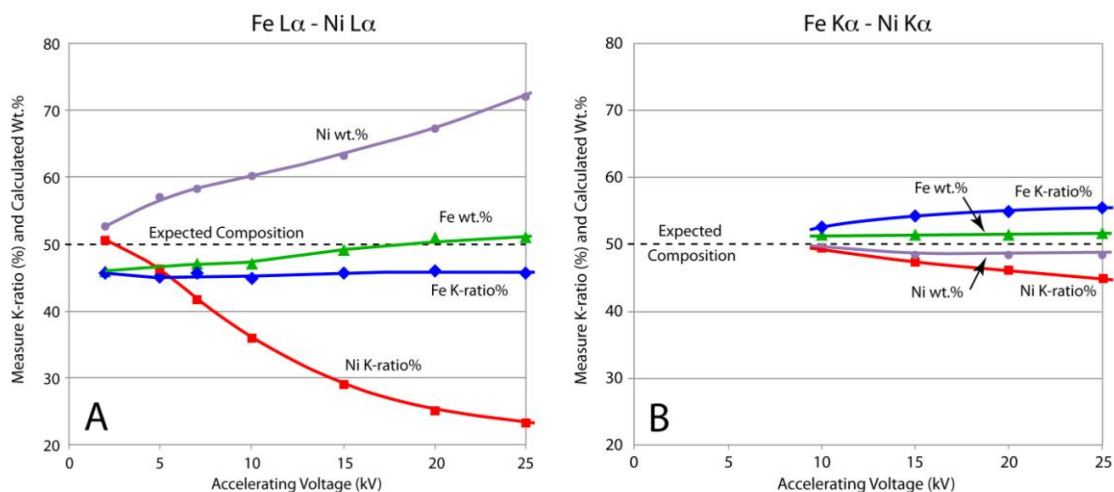


Figure 11. Measured k-ratios and matrix corrected wt.% as a function of accelerating voltage for Fe Lα and Ni Lα (A) and for Fe Kα and Ni Kα (B) for a metal containing 50 wt.% Fe and 50 wt.% Ni. Pure end-member compositions were used as standards.

For quantitative analyses of sub-micron grains, the low overvoltage method works better in the Fe-Ni system because the K lines perform better in the matrix corrections. However, analyses using the L lines can be improved by using standards that are closer to the "unknown" in composition. Table 2 compares the results of three metals along the Fe-Ni binary. Consistently the 10 kV Kα analyses are better than those of 7 kV Lα analyses using 100% metals for standards. However, the Ni Lα results are greatly improved when a 50% Ni standard is used.

Table 2. Quantitative analyses of three materials along the Fe-Ni binary using different X-ray lines, accelerating voltages, and standards.

| Weight % Ni | | | | |
|---|---|---|---|---|
| Material | 7 kV Lα 100% Ni Std | 7 kV Lα 50% Ni Std | 10 kV Kα 100% Ni Std | Expected |
| Ni35 | 43.09 | 36.34 | 35.58 | 35.32 |
| Ni25 | 30.99 | 25.98 | 24.84 | 25.18 |
| Ni15 | 19.13 | 15.88 | 16.14 | 15.17 |

| Weight % Fe | | | | |
|---|---|---|---|---|
| Material | 7 kV Lα 100% Fe Std | 7 kV Lα 50% Fe Std | 10 kV Kα 100% Fe Std | Expected |
| Ni35 | 62.81 | 66.44 | 64.42 | 64.09 |
| Ni25 | 72.62 | 76.84 | 75.16 | 75.09 |
| Ni15 | 84.05 | 88.99 | 83.86 | 84.65 |

## 9. SURFACE COATINGS

Quantitative analyses at low kV can be very sensitive to surface coatings. Figure 12 shows the effect of various carbon coat thicknesses on the intensity of the Fe Kα and Fe Lα X-rays when compared to an uncoated Fe standard. Plotted are both the calculated curves using the equation of Reed (1997), assuming a density of 1.8 gm/cc for carbon, and the measured values (red dots) from an iron standard with an approximately 15 nm carbon film. These results show close agreement between the measured and calculated values. One can then interpolate the amount of error that will result when different thicknesses of carbon are used on the standard versus the unknown.

At high accelerating voltages, when using the Fe Kα line, the difference in counts between a coated and uncoated sample is in the 0.5 wt.% range. However, at 10 kV, a standard with a 10 nm coating and an unknown with a 30 nm coating will result in a difference of up to 4 wt.% in Fe Kα counts. For the Fe Lα line (Fig. 12B), the impact of the carbon coating is much greater. At 7 kV there will be approximately a 10 wt.% difference in X-ray counts between iron samples coated with 10 nm of carbon versus 30 nm.

Similar impacts can be expected as a result of oxide layers on sulfide minerals, sputtered metal coatings, or residue from polishing. To minimize these effects, make sure the surface of both the standard and the unknown are recently polished and clean, and that any

deposited coatings are applied simultaneously to the standards and unknowns to ensure consistency.

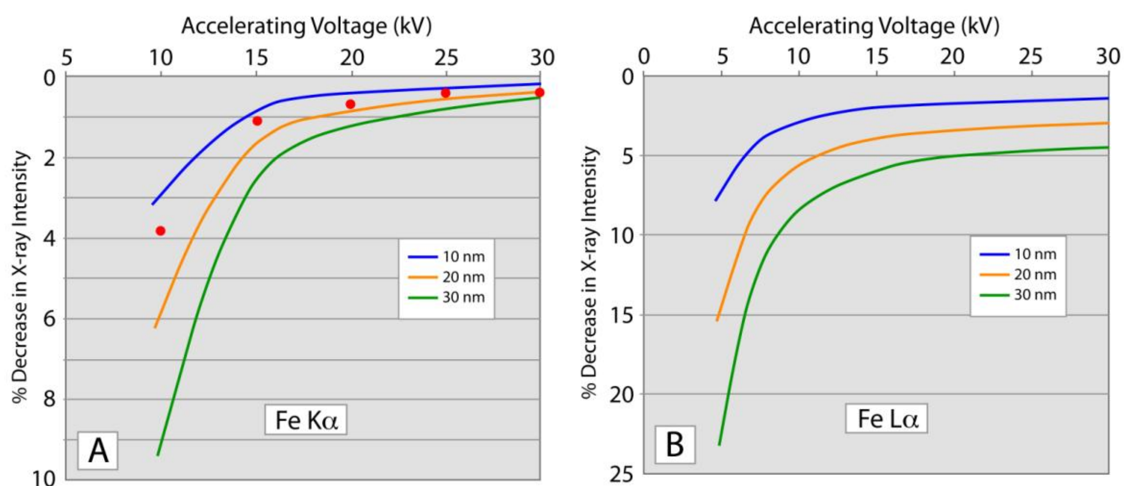


Figure 13. Effect of carbon coating on X-ray intensity. Plotted are the calculated curves showing the decrease in X-ray Fe counts resulting from carbon films that are 10 nm, 20 nm and 30 nm thick, with a density of 1.8 gm/cc (Reed, 1997, p. 157). The red dots are measured values from an iron metal standard which was expected to have about 15 nm of carbon on it surface.

## 10. CONCLUSIONS

Using either the L lines and a low accelerating voltage, or the K lines and a very low overvoltage will produce very small analytical volumes in the Fe-Ni binary. However, each method has its advantages and disadvantages. If the objective is to produce high-resolution X-ray maps, both methods will work equally well. If the objective is to produce the best quality quantitative analyses of the major elements, then the low overvoltage method is preferable, because of the better-understood behavior of the K X-rays lines. However, for quantitative analyses involving minor or trace elements, then one should consider using the L line, because they are less likely to be produced by secondary fluorescence, and a better resolution can be obtained.

Regardless of the methods used, care should be taken when carbon coating the samples to ensure that identical thickness are applied to both the standards and the unknowns, and the surfaces should be cleaned of any oxide layers or polishing residue.

## 11. REFERENCES


Armstrong, J.T., 2011, Low voltage and low overvoltage x-ray nanoanalysis with field emission electron microprobes and SEMs: Problems in quantitation for first-row transition elements; Abstract V31C-2538 presented at 2011 Fall Meeting, AGU, San Francisco, Calif., 5-9 Dec.

Fournelle, 2007, Problems in trace element EPMA: modeling secondary fluorescence with PENEPMA; Eos Trans. AGU, 88(52) Fall Meet. Suppl., Abstract V51A-0329.

Fournelle, Gosses, Kelly, Staffier, Waters and Webber, 2005, Secondary fluorescence corrections for EPMA: PENELOPE MC simulations; [abstract] Microsc. Microanal., vol. 11, Suppl. 2, p.1282-1283.

Goldstein, J.I, D.E. Newbury, P. Echlin, D.C. Joy, A.D. Romig, Jr., C. E. Lyman, C. Fiori, and E. Lifshin, 1992, Scanning Electron Microscopy and X-ray Microanalysis: a text for biologists, material scientists, and geologists; Plenum Press, 820p.

McSwiggen, P., N. Mori, M. Takakura, and C. Nielsen, 2012, Improving analytical spatial resolution with the JEOL field emission electron microprobe; [abstract] Microscopy and Microanalysis, vol. 17, Suppl. 2.

Reed, S.J.B., 1997, Electron Microprobe Analysis; Cambridge University Press, 326p.